Systematic Study of Oxo, Peroxo, and Superoxo Isomers of 3d-Metal Dioxides and Their Anions

G. L. Gutsev,* B. K. Rao, and P. Jena

Physics Department, Virginia Commonwealth University, Richmond, Virginia 23284-2000

Received: June 21, 2000; In Final Form: September 7, 2000

The electronic and geometrical structures of the ground and excited states of the 3d-metal dioxides ScO_2, TiO_2, VO_2, CrO_2, MnO_2, FeO_2, CoO_2, NiO_2, CuO_2, and ZnO_2 along with their singly charged negative ions have been calculated using the density functional theory with generalized gradient approximation for the exchange-correlation potential. We have considered oxo, peroxo, and superoxo isomers in both neutral and anionic series. The ground states of all 3d-metal dioxides and their anions possess oxo forms, except for copper dioxide, which prefers a superoxo form. All the dioxides have a large number of isomers closely spaced in total energy. The champion, FeO_2^-, possesses five isomers within an energy range of 0.35 eV. The energy gap between oxo, peroxo, and superoxo isomers decreases along the series from TiO_2 to ZnO_2. ScO_2 has peroxo and superoxo isomers which are close in total energy to its oxo ground state. The electron affinities are computed for all types of isomers and are compared to available experimental data. On the average, our theoretical values are within 0.2 eV from the corresponding experimental data. All the ground-state dioxides and their anions are found to be thermodynamically stable except for ZnO_2, which is unstable toward dissociation of molecular oxygen.

Introduction

Transition metal oxides constitute one of the most fascinating classes of inorganic solids, exhibiting a very wide variety of structures, properties, and phenomena.[1] While the structure and properties of bulk 3d-metal oxides are rather well studied,[1,2] not much is known about the structure and properties of the gas-phase 3d transition metal oxide particles. The latter are widely used in homogeneous catalysis[3] and in particular for oxidation of halocarbons.[4,5]

Experimentally,[6,7] the ground states and spectroscopic constants of the 3d-metal monoxides from ScO to ZnO have been obtained in the gas phase. Experimental investigations of 3d-metal dioxides, however, have mainly been performed under conditions of matrix isolation using electron-spin resonance (ESR)[8−15] and infrared (IR)[16−30] spectroscopies. The ESR data have been used to predict a linear symmetric geometry for MnO_2[11] that contradicts a recent observation of a bent configuration of this dioxide.[25] Another controversial example represents copper dioxide. While ESR experiments[12,13] attributed it a bent end-on structure, laser-induced emission,[31] photoexcition[32] and photolysis[33] data are consistent with a linear symmetric configuration of CuO_2. Assignment of a bent end-on structure of CuO_2 was based on observations of inequivalent oxygens; however, Mattar and Ozin[34] have shown that oxygens could be magnetically nonequivalent even at a symmetric configuration of this dioxide.

Andrews and co-workers[19−30] have produced all the 3d-metal dioxides (from ScO_2 to ZnO_2), in reactions of laser-ablated transition metal atoms with oxygen molecules in condensing inert gases. They have measured the IR spectra of isotope-substituted species and assigned vibrational frequencies based on the analysis of isotope-multiplet splittings and the results of theoretical calculations performed by different post-Hartree−Fock (HF) and density-functional theory (DFT) methods. However, their matrices have contained a large number of various species in unknown charge states that greatly complicate an unambiguous assignment because neutral, positively, and negatively charged states of the same species might have similar isotope-substitution patterns. Thus, vibrational frequencies attributed initially to ScO_2[21] have been reassigned later to ScO_2^-.[19] Comparison to theoretical vibrational frequencies is also somewhat complicated. First, vibrational frequencies of monoxides trapped in matrices are shifted with respect to their values measured in the gas phase by 10−20 cm^{-1}.[21−30] Such shifts are unknown for dioxides because there are no data on their gas-phase vibrational frequencies. Second, standard theoretical calculations provide harmonic vibrational frequencies, and anharmonic corrections should be taken into account when theoretical frequencies are to be compared with experimental values.

Since various experimental studies have been performed using different methods for producing 3d-metal dioxides followed by their trapping into inert gas matrices, considerable variations in the values of measured vibrational fundamentals have been observed. For example, the ν_1 fundamental (symmetric stretch) of CrO_2 was found to be 935,[35] 960,[18] 914,[24] and 895 ± 20 cm^{-1},[36] respectively. Similarly, the ν_3 fundamental (asymmetric stretch) was found to be 978,[35] 971,[37] 964,[38] 970,[18] and 965 cm^{-1}.[24] Thus, the frequencies measured under different experimental conditions differ by as much as 50 cm^{-1}. Even larger differences are observed between results of calculations by using different post-HF and DFT methods[19] with basis sets of approximately equal quality. For example, Chertihin et al.[24] have computed the above vibrational frequencies of CrO_2 to be 1025 and 1071 cm^{-1}, while we have obtained smaller values of 968 and 998 cm^{-1}, respectively.

During the past five years, all the 3d-metal dioxide anions, except for ZnO_2^-, have been probed[36,39−46] by laser photoelectron spectroscopy. This experimental technique provides rather accurate values of binding energies of the extra electron attached

10.1021/jp002252s CCC: $19.00
Published on Web 12/01/2000

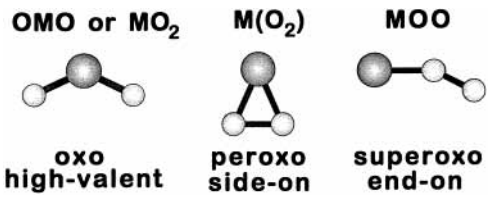

Figure 1. Structure of three types of dioxide isomers.

in the anions. Besides, photoelectron spectra contain information concerning electronically and vibrationally excited states. Thus, additional data (such as vibrational frequencies) on the structure of an anion and its neutral parent can be obtained from photoelectron spectra[47]. Some previous estimates of electron affinities of 3d-metal dioxides have been obtained from mass spectrometry experiments, e.g., for VO_2.[48] However, the latter technique provides usually much larger uncertainty bars than the laser electron spectroscopy does.

The properties of neutral 3d-metal monoxides have been computed by using several post-HF methods,[49] including the infinite-order coupled-cluster method with all singles and doubles and noniterative inclusion of triple excitations [CCSD(T)].[50] The anions of the 3d-metal monoxides were computed recently[51] by DFT methods and by a hybrid Hartree−Fock density-functional-theory method (HFDFT)[52−55] with the so-called B3LYP exchange-correlation potential.[56,57] No similar systematic calculations have been reported on the 3d-metal dioxides or their anions. Although all of the neutral dioxides have been computed[19−30,58−75] at different levels of theory including HF, post-HF, and B3LYP methods, only a few papers of Andrews and co-workers[25−29] and some others[68,69,71] have addressed the structure of isomers with different types of oxygen bonding.

Theoretical studies on the structure of the 3d-metal dioxide anions are rather scarce. Some of these studies have been performed by using DFT methods, namely, ScO_2^-,[19,21] TiO_2^-,[58] MnO_2^-,[42] and FeO_2^-.[76] The ScO_2^- anion was computed also by the CCSD[T] and CASPT2 methods,[19] and the FeO_2^- anion was computed at the MBPT^2 level.[77] The latter level failed to produce any state of the FeO_2^- anion stable toward autodetachment of the extra electron.

The aim of the present study is to calculate the structure and properties of 3d-metal dioxides and their anions systematically at the same level of theory which proved to be rather reliable in our previous calculations.[42,51,76,78−81] on the electronic and geometrical structures of 3d-metal compounds. Since oxygen can be bound to a transition metal in several ways, namely, dissociatively (typical O−O distances are around 2.5−2.8 Å) or associatively in either a peroxo (typical O−O distances are around 1.4−1.55 Å) or a superoxo (typical O−O distances are around 1.3 Å) form, we have considered all three types (see Figure 1) of isomers in both neutral and anionic series. Note that several different names are used in the literature: oxo forms are also called inserted, high-valent, or η^0-complexes; peroxo forms are named as side-on, cyclic, or η^2-complexes; superoxo forms are called end-on or η^1-complexes.[82] Since the ground state of CuO_2 has a superoxo form, it is interesting to track the evolution of oxo, peroxo, and superoxo isomers along both the neutral and anionic series. In addition, we compute adiabatic electron affinities of the neutral 3d-metal dioxides, we compute the vertical binding energies of an extra electron in the corresponding anions, and finally we evaluate the thermodynamic stability of the 3d-metal dioxides.

We have computed a number of isomers inside each oxo, peroxo, and superoxo series when searching for the lowest energy structures. Tables presented in this work contain results of calculations of the lowest energy isomers and figures show total energy shifts of excited states stable toward dissociation with respect to the corresponding ground states of neutral 3d-metal dioxides. The present calculations should be considered as a first approximation to the correct solution, and higher levels of theory and more sophisticated basis sets need to be employed to unquestionably assign the lowest energy states in these systems.

Computational Details

In our previous study[51] of the structure of 3d-metal monoxides and their anions, the exchange-correlation potential was constructed using three different generalized gradient approximations: (1) Becke's exchange[83] and Perdew−Wangs' correlation[84] functionals (BPW91), (2) Becke's exchange[83] and Lee−Yang−Parr correlation[85] functionals (BLYP), and a hybrid HFDFT approach[52−57] (B3LYP). It was found that the largest deviations from experimental values for the bond lengths are as follows: BPW91, +0.018 Å (at MnO); BLYP, +0.023 Å (at NiO); B3LYP, +0.043 Å (at CuO); and CCSD(T), +0.047 Å (at CuO). Harmonic vibrational frequencies show the following largest deviations from the experimental values: BPW91, +58 cm^{-1} (at MnO); BLYP, −62 cm^{-1} (at ZnO); B3LYP, −145 cm^{-1} (at NiO); CCSD[T], −68 cm^{-1} (at CuO). Overall, the BPW91 method appears to provide the most consistent results; thus, we have chosen this method for performing calculations for 3d-metal dioxides as well.

The calculations are performed using the molecular orbital theory where linear combinations of atomic orbitals (MO-LCAO) centered at various atomic sites constitute molecular orbitals. For the atomic orbitals we have used the standard 6-311+G* basis (Sc to Zn, [10s7p4d1f]; O, [5s4p1d]) due to Wachters[86] and Hay[87] as implemented in the Gaussian 94 software.[88] Extensive geometry optimizations were performed starting with various guess geometrical and electronic configurations for each spin multiplicity for both neutral and anionic dioxides of the oxo, peroxo, and superoxo forms. We have raised the spin multiplicity values until the states optimized are stable toward dissociation. In each case, the geometry optimization was carried out by examining the gradient forces at atomic sites and moving the atoms along the path of steepest descent until the maximum force fell below 3×10^{-4}. We feel quite confident that we are able to arrive at the lowest energy configurations within each particular isomer type.

Results and Discussion

We discuss the geometrical parameters (bond lengths and bond angles), harmonic vibrational frequencies, dipole moments, and spin multiplicities of the lowest energy configurations of each of the three isomeric forms: oxo (OMO), peroxo [$M(O_2)$], and superoxo (MOO). First we present the results for the ground states of neutral 3d-metal dioxides. This is followed by similar results on the higher energy isomers. The spin multiplicity, electron affinity, and thermodynamic stability are discussed later. The results are compared with other available theories and experiments.

Ground States of Neutral 3d-Metal Dioxides. In Table 1, we present the results for the ground states of the 3d-metal dioxides, which have the oxo form except for copper-dioxide. The latter assumes a superoxo form. Table 2 provides the electronic configurations and energy shifts of low-lying states of the oxo isomers. We begin with the results on ScO_2. This

TABLE 1: Equilibrium Bond Lengths (R_e, in Å), Bond Angles ($\angle$(OMO), in deg), Harmonic Vibrational Frequencies (ω, in cm^{-1}), and Dipole Moments (DM, in D) of the Ground-State 3d-Metal Dioxides[a]

	ScO_2		TiO_2		VO_2		CrO_2		MnO_2	
	TW $^2B_2$	ref 21 $^2B_2$	TW $^1A_1$	ref 58 $^1A_1$	TW $^2A_1$	ref 23 $^2B_1$	TW $^3B_1$	ref 24 $^3B_1$	TW $^4B_1$	ref 25 $^4B_1$
R_e	1.774	1.782	1.651	1.641	1.613	1.612	1.602	1.586	1.597	1.581
$\angle$(OMO)	129.2	125.9	110.5	111.9	110.3	121	122.4	125	128.8	131
$\omega(a_1)$	129	115	340	341	325	311	250[b]	276	261	267
$\omega(b_2)$	549	545	945	986	977	1010	998	1071	1012	1070
expt(ν_3)			935[c]		936		965		948	
$\omega(a_1)$	741	742	984	1032	996	1023	968	1025	918	947
expt(ν_1)	740 (80)[d]		962[c]		946		914		816	
DM	5.29		6.62		5.40		4.41		2.40	

	FeO_2		CoO_2		NiO_2		CuO_2		ZnO_2	
	TW $^3B_1$	ref 66 $^3B_1$	TW $^2A_1$	ref 27 $^2\Delta_g$[e]	TW $^1\Sigma_g^+$[e]	ref 28 $^1\Sigma_g^+$	TW $^2A''$[f]	ref 73 $^2A''$	TW $^3\Sigma_g^-$[e]	ref 30 $^3\Sigma_g^-$[e]
R_e	1.587	1.582	1.578		1.608	1.613	1.896	1.910	1.749	1.742
$\angle$(OMO)	137.9	141.5	154.5	180	180	180	119.3	106	180	180
$\omega(a_1)$	198	194	116	138	71	48	237	220	166	122
$\omega(b_2)$	1019	958	1042	896	1038	1027	431	535	755	821
expt(ν_3)	946		954		955		548, 530 (30)[d]		748	
$\omega(a_1)$	910	891	895	611	819	805	1184	1161	587	634
expt(ν_1)	797		772		750 (30)[d]		1089			
DM	2.02		1.11		0.0		3.12	7.26	0.0	

[a] Unless otherwise stated, the experimental data are from papers of Andrews and co-workers.[21−30] "TW" stands for "this work". The ground states of all these dioxides have the oxo form with the only exception of CuO_2, which possesses a superoxo form. Theoretical methods applied are as follows. ScO_2, BP86;[21] TiO_2, B3LYP;[58] VO_2, B3LYP;[23] CrO_2, B3LYP;[24] MnO_2, B3LYP;[25] FeO_2, B3LYP;[66] CoO_2, CASSCF;[27] NiO_2, LSDA-WVN;[28] CuO_2, MRCISD;[73] ZnO_2, B3LYP.[30] [b] Experimental value[36] is 220 ± 20. [c] See ref 9. [d] See ref 47. [e] The frequency designations are $\omega(\pi_u)$, $\omega(\sigma_g)$, and $\omega(\sigma_u)$, respectively. [f] The superoxo type: R(Cu−O) = 1.896 Å, R(O−O) = 1.289 Å, $\angle$(CuOO) = 119.3°. All frequencies have a′ symmetry.

TABLE 2: Ground and Closely Spaced States of Neutral and Negatively Charged Dioxides from ScO_2 To NiO_2, Having Oxo Forms, along with Their Electronic Configurations[a]

	neutral			anion	
	state	configuration		state	configuration
ScO_2	$^2B_2$(0.0)	$9a_1^2 1a_2^2 3b_1^2 6b_2^1$	ScO_2^-	$^1A_1$(−2.04)	$9a_1^2 1a_2^2 3b_1^2 6b_2^2$
				$^3B_2$(−1.11)	$10a_1^1 1a_2^2 3b_1^2 6b_2^1$
TiO_2	$^1A_1$(0.0)	$9a_1^2 1a_2^2 3b_1^2 6b_2^2$	TiO_2^-	$^2A_1$(−1.48)	$10a_1^1 1a_2^2 3b_1^2 6b_2^2$
VO_2	$^2A_1$(0.0)	$10a_1^1 1a_2^2 3b_1^2 6b_2^2$	VO_2^-	$^1A_1$(−1.27)	$10a_1^2 1a_2^2 3b_1^2 6b_2^2$
				$^3A_1$(−1.64)	$11a_1^1 10a_1^1 1a_2^2 3b_1^2 6b_2^2$
CrO_2	$^3B_1$(0.0)	$10a_1^1 1a_2^2 4b_1^1 6b_2^2$	CrO_2^-	$^2B_1$(−1.53)	$10a_1^2 1a_2^2 4b_1^1 6b_2^2$
				$^4B_1$(−2.22)	$11a_1^1 10a_1^1 1a_2^2 4b_1^1 6b_2^2$
MnO_2	$^4B_1$(0.00)	$11a_1^1 10a_1^1 1a_2^2 4b_1^2 6b_2^1$	MnO_2^-	$^3A_1$(−1.70)	$11a_1^1 10a_1^1 1a_2^2 4b_1^2 6b_2^2$
				$^5B_2$(−2.01)	$11a_1^1 10a_1^1 2a_2^1 4b_1^1 6b_2^2$
	$^2B_1$(0.46)	$10a_1^2 1a_2^2 4b_1^1 6b_2^2$		$^1A_1$(−1.31)	$10a_1^2 1a_2^2 4b_1^2 6b_2^2$
				$^3B_1$(−1.85)	$11a_1^1 1a_2^2 4b_1^1 6b_2^2$
FeO_2	$^3B_1$(0.00)	$11a_1^1 1a_2^1 4b_1^1 6b_2^2$	FeO_2^-	$^2B_1$(−2.15)	$11a_1^2 1a_2^1 4b_1^1 6b_2^2$
				$^4B_2$(−2.27)	$11a_1^1 2a_2^1 4b_1^1 6b_2^2$
	$^3A_1$(0.03)	$11a_1^1 10a_1^1 1a_2^2 4b_1^2 6b_2^2$		$^2A_1$(−2.21)	$11a_1^1 1a_2^2 4b_1^2 6b_2^2$
				$^4A_2$(−2.22)	$11a_1^1 10a_1^1 2a_2^1 4b_1^2 6b_2^2$
	$^5B_2$(0.05)	$11a_1^1 10a_1^1 2a_2^1 4b_1^1 6b_2^2$		$^6A_1$(−1.92)	$11a_1^1 10a_1^1 2a_2^1 4b_1^1 7b_2^1$
CoO_2	$^2A_1$(0.00)	$11a_1^1 1a_2^2 4b_1^2 6b_2^2$	CoO_2^-	$^1\Sigma_g^+$(−2.77)	$7\sigma_g^2 5\sigma_u^2 3\pi_u^4 1\pi_g^4 1\delta_g^4$
				$^3A_2$(−2.52)	$11a_1^1 2a_2^1 4b_1^2 6b_2^2$
	$^4A_2$(0.27)	$11a_1^1 10a_1^1 2a_2^1 4b_1^2 6b_2^2$		$^3A_1$(−1.37)	$11a_1^1 10a_1^1 2a_2^2 4b_1^2 6b_2^2$
	$^6A_1$(0.74)	$11a_1^1 10a_1^1 2a_2^1 4b_1^2 7b_2^1$		$^5A_1$(−2.46)	$11a_1^1 2a_2^1 4b_1^1 7b_2^1$
NiO_2	$^1\Sigma_g^-$(0.00)	$7\sigma_g^2 5\sigma_u^2 3\pi_u^4 1\pi_g^4 1\delta_g^4$	NiO_2^-	$^2A_2$(−3.25)	$11a_1^2 2a_2^2 4b_1^2 6b_2^2$
	$^3A_2$(0.07)	$11a_1^2 2a_2^1 4b_1^2 6b_2^2$		$^4\Sigma_g^-$(−3.10)	$7\sigma_g^1 5\sigma_u^2 3\pi_u^4 2\pi_g^2 1\delta_g^4$
	$^5A_1$(0.33)	$11a_1^2 2a_2^1 4b_1^1 7b_2^1$		$^6A_1$(−0.35)	$12a_1^1 11a_1^1 2a_2^1 4b_1^1 7b_2^1$

[a] Relative energy shifts (in eV) of isomers with respect to the corresponding ground states [denoted as (0.0)] are given in parentheses.

has been studied previously[21] by a DFT method using a combination of Becke's exchange[83] and Perdew's correlation[89] functionals (called BP86). The BP86 level provides ground state symmetry, geometrical parameters, and vibrational frequencies

TABLE 3: Equilibrium Bond Lengths (R_e, in Å), Bond Angles ($\angle$(OMO), in deg), and Harmonic Vibrational Frequencies (ω, in cm^{-1}) of the Ground-State 3d-Metal Dioxide Anions[a]

	ScO_2^- $^1A_1$	TiO_2^- $^2A_1$	VO_2^- $^3A_1$	CrO_2^- $^4B_1$	MnO_2^- $^5B_2$	FeO_2^- $^4B_2$	CoO_2^- $^1\Sigma_g^+$ [b]	NiO_2^- $^2A_2$	CuO_2^- $^3\Sigma_g^-$ [b]	ZnO_2^- $^2\Pi_g$ [b]
R_e	1.812	1.683	1.658	1.651	1.663	1.642	1.617	1.654	1.709	1.760
$\angle$(OMO)	126.0	111.5	120.8	134.9	126.3	129.8	180.0	170.4	180.0	180.0
$\omega(a_1)$	187	319	292	235	240	173	19	50	183	170
$\omega(b_2)$	692[c]	879[d]	904[e]	918	873	890	991	922	652	599
$\omega(a_1)$	766	915	904[e]	862	827	834	828	755	813[f]	712

[a] The B3LYP results (for the same states as given in the table): ref 19, ScO_2^-: $\omega(a_1) = 188$, 783, $\omega(b_2) = 728$; ref 58, TiO_2^-: $R_e = 1.674$, $\angle$(OMO) = 113.4, $\omega(a_1) = 319$, 956, $\omega(b_2) = 916$; ref 23, VO_2^-: $R_e = 1.655$, $\angle$(OMO) = 124.0, $\omega(a_1) = 284$, 923, $\omega(b_2) = 921$; ref 29, CuO_2^-: $R_e = 1.703$, $\angle$(OMO) = 180.0, $\omega(\pi_u) = 189$, $\omega(\sigma_g) = 673$, $\omega(\sigma_u) = 841$; ref 30, ZnO_2^-: $R_e = 1.742$, $\angle$(OMO) = 180.0, $\omega(\pi_u) = 122$, $\omega(\sigma_g) = 634$, $\omega(\sigma_u) = 821$. [b] The frequency designations are $\omega(\pi_u)$, $\omega(\sigma_g)$, and $\omega(\sigma_u)$, respectively. [c] Experimental ν_3 fundamental is 722.5.[19] [d] Experimental ν_3 fundamental is 878.[22] [e] Experimental fundamentals are 862.9 and 861.1.[23] [f] Experimental value is 887.[28]

similar to ours. This is not surprising since the BPW91 exchange-correlation functional used here is not very different from the BP86 functional. Our value of 741 cm^{-1} (see Table 1) for the symmetric stretch mode (ν_1 fundamental) fits the center of the experimental estimate of 740 ± 80 cm^{-1} deduced[47] from photoelectron spectra of ScO_2^-. The band at 722.5 cm^{-1}, attributed initially to ScO_2,[21] was reassigned in a subsequent paper[19] as due to ScO_2^-.

Schaefer et. al.[58] have found the ground state of TiO_2 to be $^1A_1$ at both B3LYP and BP86 levels of theory. Their results on vibrational frequencies show considerable improvement over those obtained in previous HF calculations.[22] Because Schaefer et al.'s BP86 results are nearly the same as ours, we present in Table 1 their B3LYP values. Ramana and Phillips[59] have obtained a similar geometry for the ground $^1A_1$ state of TiO_2 at the configuration interaction (CI) level, but they did not provide vibrational frequencies. Experimental vibrational frequencies (ν_3 = 935 cm^{-1} and ν_1 = 962 cm^{-1}) obtained by Andrews et al.[22] are in good agreement with our BPW91 frequencies of 945 and 984 cm^{-1}, respectively (see Table 1). The value of ν_1 obtained from photoelectron spectra[47] is 940 ± 40 cm^{-1}. The B3LYP frequencies[58] are somewhat larger and are in less satisfactory agreement with the experiment.

The first theoretical study[62] of VO_2 performed by the CASSCF method had predicted its ground state to be $^2A_1$. Subsequent B3LYP calculations[23] have favored a $^2B_1$ state as its ground state. The results of our BPW91 calculations are similar to those obtained using CASSCF: the ground state is $^2A_1$, and our calculated bond length of 1.61 Å and bond angle of 110.3° agree very well with the CASSCF result[62] of 1.65 Å and 110.5°, respectively. Wang[47] has deduced 970 ± 40 cm^{-1} for the symmetric stretch mode of VO_2, which is to be compared to our value of 996 cm^{-1}. Our vibrational frequencies (see Table 1) are in reasonable agreement with the IR experimental fundamentals[23] as well.

The ground state of CrO_2 is $^3B_1$ according to our BPW91/6-311+G* and Andrews et al.[24] B3LYP/6-311G* calculations. While geometrical parameters obtained at both levels are similar (see Table 1), the BPW91 vibrational frequencies are appreciably lower than the B3LYP ones and are in better agreement with both experimental fundamentals[24] obtained from the IR spectra and those estimated from photoelectron spectra of CrO_2^- by Wenthold et al.[36] The experimental fundamentals ν_1 = 895 ± 20 cm^{-1} and ν_2 = 220 ± 20 cm^{-1} have to be compared to our values of 968 and 250 cm^{-1} and the B3LYP values of 1025 and 276 cm^{-1}, respectively.

Both BPW91 and B3LYP calculations predict $^5B_1$ to be the ground state of MnO_2. Again, the B3LYP vibrational frequencies are somewhat larger than the BPW91 ones. The latter are overestimated with respect to experimental data by as much as 100 cm^{-1} (for the ν_1 fundamental). Our value of 918 cm^{-1} has to be compared to the IR value of 816 cm^{-1} [25] or 800 ± 40 cm^{-1} obtained from photoelectron spectra.[42]

There was a controversy with respect to the ground state of FeO_2.[26,66,76] B3LYP calculations have favored a $^5B_2$ state, placing it below a $^3B_1$ state by 0.1 eV, while BP86 calculations predict the opposite order with nearly the same energy splitting.[66] RCCSD[T] calculations[26] have placed the $^3B_1$ state below the $^5B_2$ one by 0.04 eV in perfect agreement with our BPW91 results.[76] Even within such a small energy interval, there is one more intermediate state, $^3A_1$,which is higher in total energy than the ground $^3B_1$ state by 0.03 eV only (see Table 2). Andrews et al.[26] have attributed IR bands at 945.8 and 797.1 cm^{-1} to the $^3B_1$ state of FeO_2. These values are to be compared to our values of 1019 and 910 cm^{-1}, respectively. Corresponding vibrational frequencies for other closely spaced states of FeO_2 are $^3A_1$, 1002 and 899 cm^{-1}; and $^5B_2$, 932 and 895 cm^{-1}. Clearly, the ν_1 fundamental disagrees with the harmonic values of the stretching a_1 mode for all low-lying neutral $^3B_1$, $^3A_1$, and $^5B_2$ states by about 100 cm^{-1}. As seen from Table 2, the FeO_2^- anion has four states within 0.12 eV energy range. The corresponding vibrational frequencies are as follows: $^2A_1$, 971 and 853 cm^{-1}, $^2B_1$, 972 and 843 cm^{-1}, $^4A_2$, 883 and 811 cm^{-1}, $^4B_2$ (the ground state, see Table 3), 890 and 834 cm^{-1}. Clearly, experimental data are in better agreement with vibrational frequency sets of $^2A_1$ and $^2B_1$ states of the FeO_2^- anion. This example shows how difficult it is to interpret experimental findings if potentially many states closely spaced in total energy could have been trapped in matrices. Yet, we did not account for a possible presence of the FeO_2^+ cation, which possesses a number of closely spaced states as well.[82]

The ground state of CoO_2 was found to be $^2A_1$ at the BP86 level; however, the results obtained at either the B3LYP or CASSCF level disagree with this assignment.[27] The CASSCF method favors a linear symmetric geometry and $^2\Delta_g$ state. With some stipulations and bearing in mind that the ground state of the CoO_2^- anion should be Σ_g^{1+}, the ground state of CoO_2 has tentatively been assigned[27] to be $^2\Sigma_g^+$. This assignment is in agreement with an ESR prediction of a linear symmetric shape for CoO_2[15] and unpublished data of Wang (ref 36 in ref 15), which were interpreted as pertaining to a linear CoO_2 due to a specific shape of the photoelectron spectra of CoO_2^- with a strong resolved progression of ν_1. However, one could notice that FeO_2^-, isoelectronic to CoO_2, possesses a bent configuration. In addition, the CoO_2^- anion appears to be floppy because its bending π_u mode was computed to be only 19 cm^{-1} (see Table 3). Starting with an angular configuration of the neutral ground state presented in Table 1, our optimization stopped at a bent configuration of $^1A_1$ symmetry with the bond angle of 170°, which is above the linear Σ_g^{1+} configuration by 0.002 eV

only. That is, the CoO_2^- anion is floppy and predictions of its ground-state configuration are governed by the accuracy of calculations (e.g., threshold values chosen for maximum gradient forces). One could also anticipate that if the closed-shell state of the anion with the highest doubly occupied $7\sigma_g$ molecular orbital is floppy, then the neutral CoO_2 would probably be bent after removal of an electron from this MO instead of having formed a linear Σ_g^{2+} state. Indeed, all three approaches, BP86, BPW91, and B3LYP, predict the Σ_g^{2+} state to be unstable toward bending because of its imaginary π_u frequency. Our computations favors $^2A_1$ to be the ground state of CoO_2; see Table 1.

The ground state of NiO_2 was assumed to have a peroxo $^1A_1$ ground state and was computed at different post-HF levels including the CCSD[T].[69] The belief that a peroxo isomer Ni-(O_2) is the ground state of nickel dioxide was based on an early paper of Blomberg et al.[70] and an experimental IR study[16] which dealt with peroxo isotope-substituted isomers of nickel dioxide. Calculations performed[28] with the local-spin-density approximation and Vosko−Wilk−Nusair exchange-correlation potential[90] (LSDA-WVN) have provided a linear Σ_g^{1+} ground state for NiO_2 and placed a peroxo $^1A_1$ state above another peroxo $^3B_1$ state by 0.1 eV. The latter peroxo $^3B_1$ state was found[28] to be above the ground Σ_g^{1+} state by 0.73 eV. Our BPW91 results are in agreement with the LSDA-WVN results and the $^3B_1$ state lies by 0.67 eV above the Σ_g^{1+} state. Andrews et al.[28] have assigned the band at 955 cm^{-1} to the ν_3 fundamental of the Σ_g^{1+} state of NiO_2, which is to be compared to our value of 1038 cm^{-1}. As follows from Table 2, a $^3A_2$ oxo isomer of NiO_2 is above its ground state by only 0.07 eV (or 564 cm^{-1}, which is less than the values of the ground-state ν_3 and ν_1 fundamentals). This state has frequencies of 942 and 810 cm^{-1} which are in better agreement with the above experimental value and the value of 750 ± 30 cm^{-1} deduced for the ν_1 fundamental by Wang[47] from his photoelectron spectra.

The ground state of CuO_2 appears to present the most controversial subject among the whole neutral 3d-metal dioxide series. Some experimental[12,13] and theoretical[29,73,75] investigations have found the lowest state of copper dioxide to possess a superoxo form and a $^2A''$ state. A symmetric linear ($^2\Pi_g$) configuration has been claimed to be the ground state of CuO_2 in several experimental[31−33,46] and theoretical[74] studies. Peroxo doublet states $^2A_2$ [69,71] and $^2B_2$ [34] have also been claimed to be the ground states of copper dioxide. According to our BPW91 calculations, the ground state of copper dioxide is $^2A''$ and has a superoxo form in agreement with the results of calculations performed by multireference configuration interactions with singles and doubles (MRCISD)[73] and B3LYP[29,75] methods. We found the lowest peroxo state to be $^2B_2$, which is above the superoxo ground state by 0.82 eV. A $^2A_2$ state was confirmed to have an imaginary asymmetric stretch frequency in agreement with the previous B3LYP result.[75] This state has converged to the ground $^2A''$ state upon lifting the C_{2v} symmetry constraint. An asymmetric linear doublet configuration of CuO_2 has converged to a symmetric configuration with nonequivalent oxygens, as was proposed early.[34] In this configuration, one oxygen carries a magnetic moment of $+1.25\ \mu_B$, whereas another oxygen has a magnetic moment of $-0.5\ \mu_B$ which is antiferromagnetically coupled to Cu ($\mu_{Cu} = 0.25\ \mu_B$). This state is above the ground state of CuOO by 0.48 eV. Our frequencies of 431 and 1184 cm^{-1} obtained for the ground superoxo state of CuOO have to be compared to the experimental IR values[29] of 548 and 1089 cm^{-1}, respectively. B3LYP frequencies[29,75] are within several cm^{-1} of ours, and the MRCISD frequencies[73] are in somewhat better agreement with the experimental values.

The ground state of ZnO_2 was predicted to be Σ_g^{3-} at the B3LYP level. Note that the isoelectronic CuO_2^- anion has the same ground state (see Table 3). As one can see below, ZnO_2 is metastable and its decay with the evolution of molecular oxygen is exothermic (by 0.6 eV). The experimental IR ν_3 fundamental of 748 cm^{-1} is in good agreement with our value of 755 cm^{-1} (see Table 1).

In the series of 3d-metal monoxides [ScO($^2\Sigma^+$), TiO($^3\Delta$), VO($^4\Sigma^-$), CrO($^5\Pi$), MnO($^6\Sigma^+$), FeO($^5\Delta$), CoO($^4\Delta$), NiO($^3\Sigma^-$), CuO($^2\Pi$), and ZnO($^1\Sigma^+$)], the spin multiplicity increases gradually from ScO to MnO and then decreases when moving toward ZnO. That is, the monoxides have the same ground-state spin multiplicities as the corresponding transition metal atoms, except for Cr whose ground-state spin multiplicity is 7 and corresponds to a $3d^54s^1$ electronic configuration. In other words, Cr behaves "regularly" when forming the monoxide—as if it possesses a $3d^44s^2$ electronic configuration, intermediate between the neighbor V ($3d^34s^2$) and Mn ($3d^54s^2$) electronic configurations.

Adding the second oxygen atom to a 3d-metal monoxide influences seriously the ground-state spin multiplicities of the 3d-metal dioxides formed. While ScO_2 retains the same spin multiplicity as Sc and ScO have, TiO_2 reduces its spin multiplicity by 2, as do subsequent dioxides up to NiO_2. CuO_2 retains the same spin multiplicity as Cu and CuO, and finally, ZnO_2 increases its spin multiplicity with respect to singlet Zn and ZnO. Such trends are to be related to a substantial involvement of 3d electrons in chemical bonding in 3d-metal dioxides with respect to that in 3d-metal monoxides, which, in turn, results in quenching the magnetic moments at metal sites.

Ground States of 3d-Metal Dioxide Anions. Several calculations for the 3d-metal dioxide anions have been performed at the B3LYP level, namely, for ScO_2^-,[21] TiO_2^-,[58] VO_2^-,[23] CuO_2^-,[29] and ZnO_2^-.[30] The ScO_2^- and TiO_2^- anions have been computed also at the BP86 level, and these results are close to our BPW91 values, as well as those obtained at the CCSD[T] level (see refs 19 and 58). CCSD[T] calculations for TiO_2^- and TiO_2 have been performed at the geometry optimized at the B3LYP level and provided a value in good agreement with the experimental adiabatic electron affinity of TiO_2. However, attempts to optimize the structure of ScO_2^- and ScO_2 led Bauschlicher et al.[19] to a conclusion: "... it is not possible to definitely determine the geometry of ScO_2 at the CCSD[T] level of theory." We reached at the same conclusion when we have attempted to optimize the ground state of TiO_2^- at the CCSD[T] level of theory.

In Table 3, we present our results on the equilibrium bond lengths and harmonic vibrational frequencies for the ground states of the 3d-metal dioxide anions. Available B3LYP data are given in a footnote for comparison. The geometries obtained by both methods are in good agreement, whereas vibrational frequencies are not: the difference exceeds 100 cm^{-1} for ZnO_2^-. Available experimental fundamentals of the anions are in reasonable agreement with the results of our computations.

Comparing the ground states of the neutral 3d-metal dioxides and their anions in Tables 1 and 3, one can see that the majority of the anions prefer to form states whose spin multiplicity is higher by 1 than their neutral parents. Exceptions are ScO_2^-, CoO_2^-, and ZnO_2^-: ScO_2^- and CoO_2^- prefer to form closed-shell singlet states, although their triplet states are also stable toward autodetachment of an extra electron. In the whole series, only TiO_2^- possesses a sole state which is stable toward

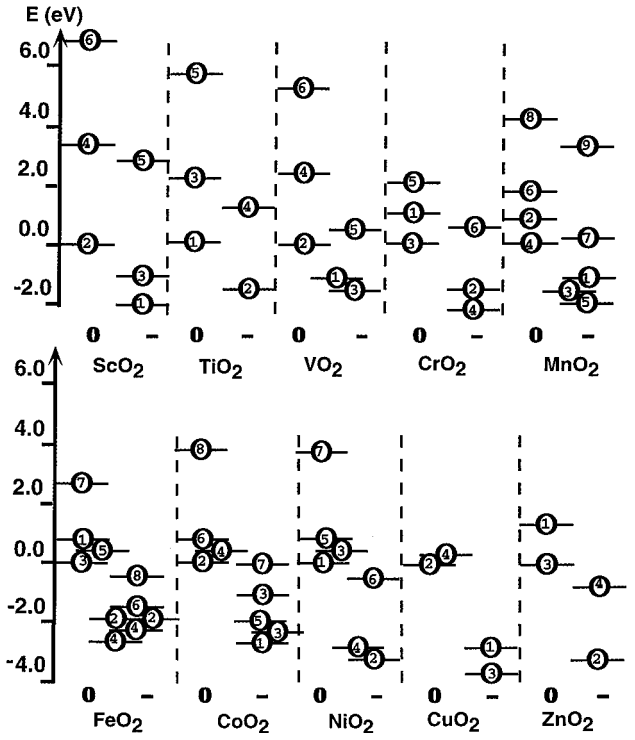

Figure 2. Energies (in eV) of oxo isomers of neutral (**0**) and anionic (−) 3d-metal dioxides given with respect to the total energy of the ground state of each particular dioxide. Numbers within the circles denote the spin multiplicity of the corresponding state.

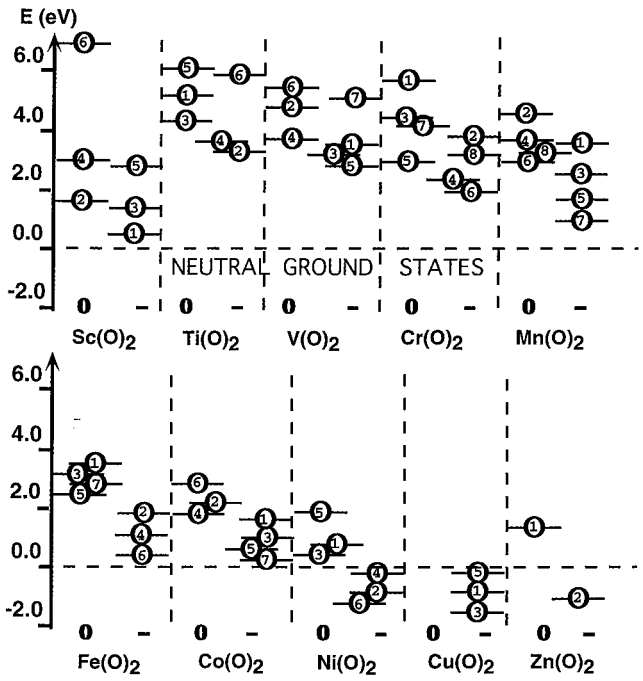

Figure 3. Energies (in eV) of the neutral (**0**) and anionic (−) peroxo isomers of 3d-metal dioxides given with respect to the total energies of the lowest oxo states of each particular neutral dioxide. Numbers within the circles denote the spin multiplicity of the corresponding state.

autodetachment of an extra electron. All other 3d-metal dioxide anions possess at least two stable states.

Figure 2 summarizes the results of our calculations on oxo isomers of 3d-metal dioxides and their ions. It presents the total energies of isomers for different spin multiplicities with respect to the total energies of the neutral ground states. As is seen, MnO_2, FeO_2, and CoO_2 and their anions possess the largest number of closely spaced isomers.

Lowest States of Peroxo Isomers. The lowest energy peroxo isomers of neutral and negatively charged 3d-metal dioxides are presented in Table 4. Previous B3LYP computations[21−30] have been performed for the neutral peroxo isomers only (except for TiO_2), and their lowest energy states are presented in the table for comparison. Since the latter computations have been aimed at interpreting experimental IR data, the authors have provided vibrational frequencies but not geometrical parameters or spectroscopic states in each case. One can see rather good agreement between the results of the BPW91 and B3LYP calculations in the beginning of the series (ScO_2, VO_2, CrO_2, and FeO_2), whereas the B3LYP approach predicts different states to be the lowest in total energy for MnO_2, CoO_2, CuO_2, and ZnO_2. Our previous computations of FeO_2 performed by both B3LYP and BPW91 levels allow us to conclude that the BPW91 method is more reliable.[76]

As is seen from comparison of entries in Tables 1 and 4, the peroxo isomers have generally higher spin multiplicities than the corresponding ground-state oxo isomers (except for copper dioxide, which has a superoxo form). The spin multiplicities corresponding to the lowest energy configurations of peroxo isomers do increase continuously from Sc to Mn and then decrease with the only exception of $Co(O_2)$, whose preferred spin multiplicity is 2 while those of $Fe(O_2)$ and $Ni(O_2)$ are 5 and 3, respectively. Let us note that a $^4B_1$ isomer of $Co(O_2)$ is higher in total energy by only 0.14 eV. The maximum spin multiplicity in the peroxo series belongs to $Mn(O_2)$, and its spin multiplicity is the same as that of Mn atom in its ground state.

No calculations have been reported for the peroxo anions $M(O)_2^-$, whereas some of them were observed in photodetachment spectra.[47] In Figure 3, we plot the energies of the neutral and negatively charged peroxo isomers for different spin multiplicities. Note that peroxo anion isomers from $Sc(O_2)^-$ to $Co(O_2)^-$ are metastable with respect to autodetachment to the neutral ground states while $Ni(O_2)^-$ and $Cu(O_2)^-$ possess three stable isomers and $Zn(O_2)^-$ has one stable isomer.

Lowest States of Superoxo Isomers. The results of calculations on the lowest energy superoxo isomers are displayed in Table 5. As is seen, the spin multiplicities of superoxo isomers are the same as those of the peroxo isomers (see Table 4) except for NiOO, which prefers a singlet state. The energy gap between total energies of the ground states and corresponding superoxo isomers is decreasing along the 3d-metal dioxide series up to CuOO, whose ground state is of the superoxo type. Previous calculations have been performed by the B3LYP method for CrOO, MnOO, FeOO, and NiOO (see footnote in Table 5). The results of our calculations agree with those obtained using B3LYP for CrOO and NiOO. Unlike the peroxo and similar to oxo isomers, the superoxo isomers prefer to form low-spin anion states upon attachment of an extra electron. All superoxo isomers can attach an extra electron and form a metastable anion state of the superoxo type.

Figure 4 shows the energetic positions of the superoxo isomers of the neutral and negatively charged 3d-metal dioxides relative to the total energies of the corresponding ground-state species. The energy gap between the lowest energy superoxo isomers decreases for both neutrals and anions as one proceeds from Ti to Zn. Finally, CuOO is below its linear oxo isomer and $NiOO^-$, $CuOO^-$, and $ZnOO^-$ have isomers stable with respect to autodetachment of an extra electron. They are stable toward fragmentation as well.

Magnetic Moments. While the charges on atoms in 3d-metal dioxides are similar to those found for 3d-metal monoxides[51]and

TABLE 4: Equilibrium Bond Lengths (R, in Å), Bond Angles ($\angle$(OMO), in deg), Harmonic Vibrational Frequencies (ω, in cm^{-1}), and Dipole Moments (DM, in D) of the Lowest Peroxo Isomers of 3d-Metal Dioxides and Their Anions[a]

	$Sc(O_2)$		$Ti(O_2)$	$V(O_2)$		$Cr(O_2)$		$Mn(O_2)$	
	TW $^2A_1$	ref 21 $^2A_1$	TW $^3A_1$	TW $^4B_1$	ref 23 $M=4$	TW $^5B_2$	ref 24 $^5B_2$	TW $^6A_1$	ref 25 $^4B_1$
R(M−O)	1.858	1.870	1.829	1.830	1.817	1.825	1.820	1.829	1.851
R(O−O)	1.491	1.494	1.459	1.420	1.420	1.465	1.456	1.550	1.390
$\angle$(OMO)	47.3	47.1	47.0	45.7	46.0	47.3	47.0	50.2	44.0
$\omega(a_1)$	638	634	665	592	629	598	608	387	393
$\omega(b_2)$	578	570	493	416	409	523	575	1265	1020
$\omega(a_1)$	869	882	915	949	942	887	919	772	390
DM	4.19		4.59	4.40		5.92		6.17	
ΔE_{tot}	1.57	1.43	4.46	3.85		3.26	2.43	3.00	2.51

	$Fe(O_2)$		$Co(O_2)$		$Ni(O_2)$		$Cu(O_2)$		$Zn(O_2)$	
	TW $^5A_1$	ref 66 $^5A_1$	TW $^2A_2$	ref 27 $^4A_1$	TW $^3B_1$	ref 28 $M=3$	TW $^2B_2$	ref 73 $^2A_2$	TW $^1A_1$	ref 30 $^3A_2$
R(M−O)	1.828	1.812	1.774		1.864	1.844	1.911		1.849	2.044
R(O−O)	1.475	1.491	1.377		1.377	1.382	1.447		1.728	1.365
$\angle$(OMO)	47.6	48.6	45.7		43.4	44.0	44.5		55.8	39.0
$\omega(a_1)$	426	510	610	441	473[b]	516	414	401	438	423
$\omega(b_2)$	321	462	1231	320	198	60	161	171	521	170
$\omega(a_1)$	838	842	1007[c]	903	992[b]	1037	911	1037	682	1150
DM	5.34		3.93		4.15		4.94		6.68	
ΔE_{tot}	2.56		1.86		0.67	0.74	0.82	0.61	1.57	

	$Sc(O_2)^-$ $^1A_1$	$Ti(O_2)^-$ $^2A_1$	$V(O_2)^-$ $^3B_1$[d]	$Cr(O_2)^-$ $^6B_2$	$Mn(O_2)^-$ $^7A_1$
R(M−O)	1.894	1.864	1.858	1.895	1.906
R(O−O)	1.493	1.470	1.438	1.474	1.531
$\angle$(OMO)	46.4	46.4	45.5	45.8	47.4
$\omega(a_1)$	611	627	579	523	444
$\omega(b_2)$	519	432	212	345	447
$\omega(a_1)$	846	881	907	858	746
peroxo EA	1.03	1.00	0.79	1.29	1.82
expt	1.1				

	$Fe(O_2)^-$ $^6A_1$	$Co(O_2)^-$ $^5A_1$	$Ni(O_2)^-$ $^4B_1$	$Cu(O_2)^-$ $^3B_2$	$Zn(O_2)^-$ $^2A_1$
R(M−O)	1.884	1.887	1.914	1.981	1.929
R(O−O)	1.488	1.463	1.401	1.436	1.624
$\angle$(OMO)	46.5	45.6	42.9	42.5	49.8
$\omega(a_1)$	448	452	422	337	454
$\omega(b_2)$	435	339	76	247	377
$\omega(a_1)$	798	840	940	916	680
peroxo EA	1.78	1.64	1.35	1.65	2.73
expt			0.82	1.50	

[a] ΔE_{tot}(eV) denotes the shift in total energy with respect to the corresponding neutral ground state energy. "Peroxo EA" denotes the difference in total energy between the given anion and its neutral peroxo parent presented in the top panel. TW refers to "this work". [b] Experimental values are 504 and 966, respectively.[16] [c] Experimental value is 985.[27] [d] The lowest energy state with the multiplicity of 5 ($^5B_1$) converged to the ground-state superoxo $^5A''$ state.

iron oxides FeO_n ($n \leq 4$),[76] magnetic moments which are related to spin multiplicities are more sensitive to the composition and shape of a cluster. Our computed values of magnetic moments for all three types of isomers of neutral and negatively charged 3d-metal dioxides are summarized in Table 6.

Magnetic moments at oxygen sites in the ground states of the neutral 3d-metal dioxides are nearly zero except for ScO_2, CuO_2, and ZnO_2. The unpaired electron in is ScO_2 delocalized over oxygen atoms, which means that a 3d electron of Sc is involved in chemical bonding. The magnetic moment of Cu in CuO_2 is small and coupled antiferromagnetically to magnetic moments of oxygen atoms. Attachment of an extra electron quenches the magnetic moments in ScO_2^- because its ground state is a singlet. The magnetic moment of Cu increases and that of Zn decreases in $CuOO^-$ and $ZnOO^-$, respectively. In NiO_2^-, the magnetic moments of Ni and two oxygens are nearly the same. All the other dioxide anions show negligible changes in magnetic moments at oxygen sites due to attachment of an extra electron.

In the neutral peroxo series, the magnitudes of the magnetic moments at oxygen sites correspond to an electron localized at the O_2 group in $Fe(O_2)$, $Ni(O_2)$, and $Cu(O_2)$ only. In $Mn(O_2)$ and $V(O_2)$, the magnetic moment of O_2 is about 0.5 μ_B, and it couples antiferromagnetically to the magnetic moment of the metal atom in $V(O_2)$. Attachment of an extra electron does not lead to a significant redistribution of the spin densities at oxygen sites.

Among the superoxo isomers, magnetic moments at oxygens are antiferromagnetically coupled in the beginning of the series, namely, in ScOO, TiOO, VOO, and CrOO. The superoxo O_2 group carries approximately one unpaired electron in VOO, CrOO, CoOO, and CuOO. Surprisingly, the magnetic moments at oxygens in superoxo isomers of MnOO and FeOO are small and dioxygen behaves as an oxygen atom in MnO and FeO, respectively.

TABLE 5: Equilibrium Bond Lengths (R, in Å), Bond Angles ($\angle$(OMO), in deg), Harmonic Vibrational Frequencies (ω, in cm^{-1}), and Dipole Moments (DM, in D) of the Lowest Energy Superoxo Isomers of the 3d-Metal Dioxides and Their Anions[a]

	ScOO $^2\Sigma^+$	TiOO $^3\Pi$	VOO $^4\Sigma^-$	CrOO $^5A''$	MnOO $^6A'$
R_e	1.761	1.721	1.701	1.813	1.778
R(O−O)	1.321	1.306	1.296	1.333	1.458
$\angle$(MOO)	180.0	180.0	180.0	99.9	72.6
π, ω(a′)	209	210	194	66	371
σ, ω(a′)	592	582	558	537	583
σ, ω(a′)	1175	1219	1249	1065	800
DM	0.0	0.0	0.0	3.26	4.44
ΔE_{tot}	3.33	5.51	4.79	3.67	2.92
	$ScOO^-$ $^1\Sigma^+$	$TiOO^-$ $^2\Pi$	VOO^- $^3\Sigma^-$	$CrOO^-$ $^4A''$	$MnOO^-$ $^5A'$
R_e	1.772	1.722	1.699	1.797	1.812
R(O−O)	1.357	1.341	1.332	1.351	1.486
$\angle$(MOO)	180.0	180.0	180.0	120.3	72.3
π, ω(a′)	201	204	192	143	339
σ, ω(a′)	568	574	552	508	544
σ, ω(a′)	1094	1137	1150	1002	721
superoxo EA	1.48	1.26	1.08	0.84	1.17
	FeOO $^5A'$	CoOO $^4A'$ [b]	NiOO $^1A'$ [c]	CuOO $^2A''$	ZnOO $^1A'$
R_e	1.768	1.792	1.728	1.898	2.057
R(O−O)	1.313	1.440	1.284	1.288	1.288
$\angle$(MOO)	124.4	70.2	125.3	119.3	124.4
π, ω(a′)	148	189	288	237	199
σ, ω(a′)	523	509	597	431	350
σ, ω(a′)	1122	858	1205	1184	1196
DM	4.10	4.97	3.23	3.12	3.32
ΔE_{tot}	2.97	1.88	1.40	0.0	0.47
	$FeOO^-$ $^4A''$ [d]	$CoOO^-$ $^3A''$ [e]	$NiOO^-$ $^2A''$	$CuOO^-$ $^3A''$	$ZnOO^-$ $^2A''$
R_e	1.767	1.745	1.744	1.957	2.432
R(O−O)	1.355	1.367	1.352	1.332	1.355
$\angle$(MOO)	129.6	117.2	120.1	120.3	69.8
π, ω(a′)	171	197	229	186	40
σ, ω(a′)	470	598	575	350	196
σ, ω(a′)	1011	954	1001	1056	1094
superoxo EA	1.46	1.47	2.15	1.39	2.41

[a] ΔE_{tot} (eV) denotes the difference in total energy between a given superoxo isomer and the corresponding ground-state neutral dioxide. "Superoxo EA" denotes the difference in total energy between a given anion and its neutral superoxo parent presented in the top panel. [b] The $^2A'$ state is higher by 0.11 eV. [c] The triplet state converged to the peroxo ground state. [d] Nearly degenerate in total energy with a state of multiplicity 6 ($^6\Pi$ or $^6\Delta$). [e] $^5\Sigma^-$ state is higher by 0.05 eV. [f] Other theoretical results: CrOO(B3LYP, ref 24): $^5A''$, +2.90 eV, R_e = 1.853, R(O−O) = 1.318, $\angle$(MOO) = 104°, ω' = 128, 526, 1165; MnOO(B3LYP, ref 25: the lowest isomer is $^4A''$, the next one is $^6A''$; FeOO(B3LYP, ref 26): a quintet state has converged to a peroxo isomer; NiOO(B3LYP, ref 28): singlet, +1.47 eV, R_e = 1.721, R(O−O) = 1.302, $\angle$(MOO) = 123°, ω' = 265, 622, 1227.

Electron Affinities

The adiabatic electron affinity (A_{ad}) of a neutral molecular system is defined as the difference in the ground-state total energies of the system and its anion. Within the Born−Oppenheimer approximation used in the present work, we evaluate the A_{ad} as

$$A_{ad} = E_{tot}(MO_2,R_e) + Z(MO_2) - E_{tot}(MO_2^-,R_e^-) - Z(MO_2^-) = \Delta E_{el} + \Delta E_{nue} \quad (1)$$

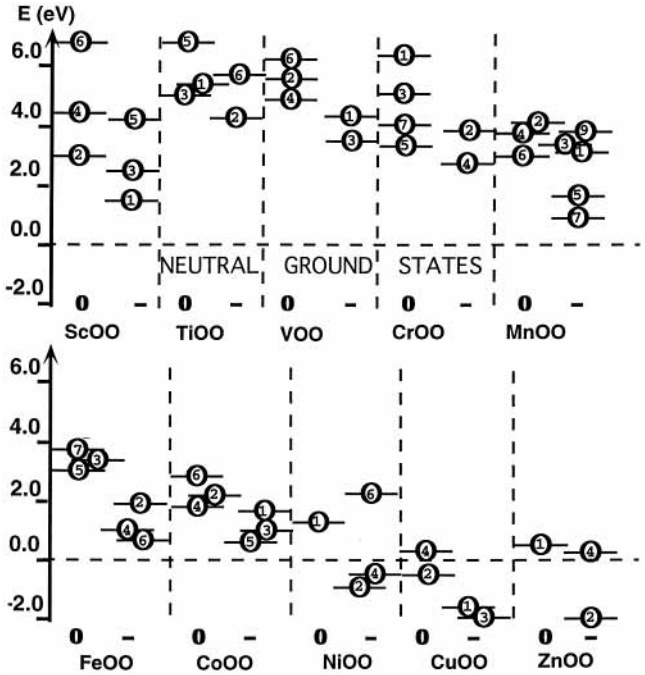

Figure 4. Energies (in eV) of the neutral (**0**) and anionic (−) superoxo isomers of 3d-metal dioxides given with respect to the total energies of the lowest oxo states of each particular neutral dioxide. Numbers within the circles denote the spin multiplicity of the corresponding state.

where R_e and R_e^- denote equilibrium geometries of a neutral dioxide (MO_2) and its anion (MO_2^-), respectively. The zero-point vibrational energies (Z) are computed within the harmonic approximation. The differences in zero-point energies ΔE_{nuc} are about 0.01 eV, they are neglected. The electron affinities (EA) estimated for peroxo and superoxo isomers in the same way are given in Tables 4 and 5. Both types of these isomers are metastable with respect to the corresponding oxo ground states (except for CuO_2, which has a superoxo ground-state configuration). A positive value of the EA of a peroxo or superoxo isomer means that a corresponding isomer is able to attach an extra electron and form an anion state which is stable toward this parent state, although it can be metastable with respect to the anion ground state. Due to barriers for geometrical transformations, such peroxo and superoxo anions could have appreciable lifetimes.

There are scarce data on electron affinities of peroxo or superoxo isomers of the 3d-metal dioxides. The values obtained by Wang[47] for $Sc(O_2)$ and $Cu(O_2)$, 1.1 and 1.5 eV, are in good agreement with our values of 1.03 and 1.65 eV, respectively. The experimental value of 0.82 eV assigned as a peroxo A_{ad} of $Ni(O_2)$ is in disagreement with our value of 1.35 eV presented in Table 4. However, there is another peroxo isomer $^4A_2$ of $Ni(O_2)$, whose presence in the ion beam may not be ruled out, with an electron detachment energy of 0.72 eV. The latter value is in good agreement with experiment.

Photoelectron spectra present vertical binding energies of electrons suddenly detached from an anion. Vertical binding energies can be computed by analogy with eq 1 as the differences in total energies at the anion equilibrium geometry:

$$E_b = E_{tot}(MO_2,R_e^-) - E_{tot}(MO_2^-,R_e^-) \quad (2)$$

The difference between an A_{ad} and the corresponding E_b is called an adiabatic correction and reflects the change in the equilibrium geometries of an MO_2 and MO_2^- pair. Because the differences in the geometries of the 3d-metal dioxide pairs are

TABLE 6: Magnetic Moments of Atoms [μ_A, in Bohr Magnetons (μ_B)] of the Ground-State Neutral and Anionic 3d-Metal Dioxides, as Well as of Their Lowest Energy Peroxo and Superoxo States[a]

	ScO_2	TiO_2	VO_2	CrO_2	MnO_2	FeO_2	CoO_2	NiO_2	CuO_2	ZnO_2
oxo	$^2B_2$	$^1A_1$	$^2A_1$	$^3B_1$	$^4B_1$	$^3B_1$	$^2A_1$	$^1\Sigma_g^+$	$^4\Sigma_g^+$	$^3\Sigma_g^+$
μ_M	−0.09	0.0	1.19	2.27	3.14	2.08	0.94	0.0	1.02	−0.07
μ_O	0.54	0.0	−0.09	−0.13	−0.07	−0.04	0.03	0.0	0.99	1.04
peroxo	$^2A_1$	$^3A_1$	$^4B_1$	$^5B_2$	$^6A_1$	$^5A_1$	$^2A_2$	$^3B_1$	$^2A_2$	$^1A_1$
μ_M	1.06	2.22	3.40	4.10	4.48	3.18	0.72	0.85	−0.02	0.0
μ_O	−0.03	−0.11	−0.20	−0.05	0.26	0.41	0.14	0.57	0.51	0.0
superoxo	$^2\Sigma^+$	$^3\Pi$	$^4\Sigma^-$	$^5A''$	$^6A'$	$^5A'$	$^4A'$	$^1A'$	$^2A''$	$^1A'$
μ_M	1.35	2.67	3.95	5.00	4.67	3.72	2.08	0.0	−0.31	0.0
μ_{O_b}	−0.16	−0.29	−0.38	−0.47	0.08	0.13	0.43	0.0	0.57	0.0
μ_{O_t}	−0.19	−0.38	−0.57	−0.53	0.25	0.14	0.49	0.0	0.74	0.0
	ScO_2^-	TiO_2^-	VO_2^-	CrO_2^-	MnO_2^-	FeO_2^-	CoO_2^-	NiO_2^-	CuO_2^-	ZnO_2^-
oxo	$^1A_1$	$^2A_1$	$^3A_1$	$^4B_1$	$^5B_2$	$^4B_2$	$^1A_1$	$^2A_2$	$^3\Sigma_u^-$	$^2\Pi_g$
μ_M	0.0	1.04	2.15	3.35	3.85	2.66	0.0	0.48	0.32	−0.08
μ_O	0.0	−0.02	−0.08	−0.17	0.07	0.17	0.0	0.26	0.84	0.54
peroxo	$^1A_1$	$^2A_1$	$^3B_1$	$^6B_2$	$^7A_1$	$^6A_1$	$^5A_1$	$^4B_1$	$^3B_2$	$^2A_1$
μ_M	0.0	1.14	2.30	5.10	5.64	4.38	3.24	2.02	1.24	0.88
μ_O	0.0	−0.07	−0.15	−0.05	0.18	0.32	0.28	0.49	0.38	0.06
superoxo	$^1\Sigma^+$	$^2\Pi$	$^3\Sigma^-$	$^4A''$	$^5A'$	$^4A''$	$^3A''$	$^2A''$	$^3A''$	$^2A''$
μ_M	0.0	1.40	2.76	3.85	3.80	3.14	1.50	0.21	0.80	−0.03
μ_{O_b}	0.0	−0.22	−0.37	−0.41	0.06	0.0	0.25	0.37	0.56	0.53
μ_{O_t}	0.0	−0.18	−0.39	−0.44	0.14	−0.14	0.25	0.42	0.64	0.50

[a] O_b and O_t denote bridge and terminal oxygen atoms, respectively, in the superoxo isomers.

TABLE 7: Adiabatic Electron Affinities (A_{ad}, in eV) of the Neutral Metal Dioxides and Vertical Binding Energies (B_e, in eV) of an Extra Electron to Neutral States with Spin Multiplicities of ($M - 1$) and ($M + 1$) from the Anion Ground States with the Spin Multiplicity M[a]

	ScO_2 $^2B_2$	TiO_2 $^1A_1$	VO_2 $^2A_1$	CrO_2 $^3B_1$	MnO_2 $^4B_1$	FeO_2 $^3B_1$	CoO_2 $^2A_1$	NiO_2 $^1\Sigma_g^+$	CuO_2 $^2A''$	ZnO_2 $^3\Sigma_g^+$
A_{ad}(TW)	2.05	1.49	1.64	2.22	2.01	2.29	2.78	3.25	3.30	3.26
A_{ad}(expt)	2.32	1.59	2.01	2.41	2.06	2.36	2.97	3.05	3.47	
	ScO_2^- $^1A_1$	TiO_2^- $^2A_1$	VO_2^- $^3A_1$	CrO_2^- $^4B_1$	MnO_2^- $^5B_2$	FeO_2^- $^4B_2$	CoO_2^- $^1\Sigma_g^+$	NiO_2^- $^2A_2$	CuO_2^- $^3\Sigma_u^-$	ZnO_2^- $^2\Pi_g$
$B_e(M-1)$	2.09	1.52	1.90	2.35	2.18	2.43		3.33	4.09	4.54
$B_e(M+1)$		3.74	4.70	4.26	3.95	2.45	2.84	3.40	3.09	3.27

[a] Experimental A_{ad}'s are from refs 21−29.

generally small, adiabatic corrections are small as well (see Table 7) except for CuO_2.

Table 7 compares theoretical values with adiabatic electron affinities evaluated from experimental photoelectron spectra. On the average, the discrepancy does not exceed 0.2 eV. The largest discrepancy is observed for the A_{ad} of VO_2 (0.36 eV), whereas the vertical detachment energy of 1.90 eV is closer to the experimental value of 2.01 eV. Note that detachment energies to the low-spin neutral states are smaller than those to the high multiplicity states for all the anions except for CuO_2 and ZnO_2. Previous theoretical estimations are known for the A_{ad} of ScO_2 and TiO_2 only. Schaefer et al.[58] have obtained values of 1.68, 1.62, and 1.60 eV at the B3LYP, BP86, and CCSD[T]/B3LYP levels, respectively, which are in good agreement with our BPW91 value of 1.49 eV. The A_{ad} of ScO_2 was computed[19] to be 2.4 and 2.0 eV at the CCSD[T] and CASPT2 levels, respectively. Our value of 2.05 eV is closer to the latter value.

Thermodynamic Stability

Experimental bond rupture energies are known for several neutral 3d-metal dioxides.[91−100] In addition to bond rupture energies, we have also computed energies required to dissociate to molecular oxygen. By definition, fragmentation energies correspond to the differences in total energies between the parent and fragments formed in a particular decay channel

$$D_0(MO_2) = \sum_i [E_{tot}(F_i) + Z_{F_i}] - E_{tot}(MO_2) - Z(MO_2) = D_e(MO_2) + \Delta Z_{nuc} \quad (3)$$

where fragments are O, O_2, and metal atoms. The zero-point energies, Z, are calculated by using the harmonic approximation.

Comparison of our computed values with the experimental data in Table 8 shows rather good agreement both in the beginning and in the end of the neutral series. There are several peculiarities in the fragmentation trends across the neutral series: (i) the most thermodynamically stable systems are d-electron-poor dioxides such as TiO_2 and VO_2; (ii) beginning with MnO_2, the evolution of molecular oxygen is energetically preferable over a single bond rupture; (iii) in the end of the series, the 3d-electron-rich CuO_2 is barely stable and ZnO_2 is even unstable toward evolution of molecular oxygen. Since ZnO_2 has a linear ground-state configuration and is thermodynamically stable toward abstraction of an atomic oxygen, its existence in a metastable state is due to the barrier toward bending.

On the whole, the anions are more stable with respect to fragmentation than their neutral parents, and NiO_2^-, CuO_2^-,

TABLE 8: Fragmentation Energies (D_0, in eV) of the Neutral 3d-Metal Ground-State Dioxides and Their Anions

channel	D_0	expt	channel	D_0	channel	D_0
$ScO_2 \rightarrow ScO + O$	4.5	3.95 ± 0.33[a]	$ScO_2^- \rightarrow ScO + O^-$	4.9	$FeO_2^- \rightarrow FeO + O^-$	5.4
$\rightarrow Sc + O_2$	6.4		$\rightarrow ScO^- + O$	5.5	$\rightarrow FeO^- + O$	5.8
$TiO_2 \rightarrow TiO + O$	6.7		$\rightarrow Sc + O_2^-$	8.0	$\rightarrow Fe^- + O_2$	5.9
$\rightarrow Ti + O_2$	8.9		$\rightarrow Sc^- + O_2$	8.2	$\rightarrow Fe + O_2^-$	6.1
$VO_2 \rightarrow VO + O$	6.1	6.33 ± 0.20[b]	$TiO_2^- \rightarrow TiO + O^-$	6.5	$CoO_2^- \rightarrow Co^- + O_2$	5.3
$\rightarrow V + O_2$	8.1		$\rightarrow TiO^- + O$	7.2	$\rightarrow Co + O_2^-$	5.7
$CrO_2 \rightarrow Cr + O_2$	5.1		$\rightarrow Ti^- + O_2$	9.6	$\rightarrow CoO + O^-$	5.8
$\rightarrow CrO + O$	6.0	$5.47^{-0.3}_{+0.65}$ [c]	$\rightarrow Ti + O_2^-$	10.0	$\rightarrow CoO^- + O$	6.0
$MnO_2 \rightarrow Mn + O_2$	4.7		$VO_2^- \rightarrow VO + O^-$	6.2	$NiO_2^- \rightarrow Ni^- + O_2$	4.6
$\rightarrow MnO + O$	5.1	4.99[d]	$\rightarrow VO^- + O$	7.0	$\rightarrow Ni + O_2^-$	5.2
$FeO_2 \rightarrow Fe + O_2$	4.3	2.94 ± 0.39[e]	$\rightarrow V^- + O_2$	8.6	$\rightarrow NiO + O^-$	5.2
$\rightarrow FeO + O$	4.8	$4.44^{-0.13}_{+0.22}$ [f]	$\rightarrow V + O_2^-$	9.3	$\rightarrow NiO^- + O$	5.6
$CoO_2 \rightarrow Co + O_2$	3.4		$CrO_2^- \rightarrow CrO + O^-$	6.6	$CuO_2^- \rightarrow Cu^- + O_2$	2.9
$\rightarrow CrO + O$	4.7		$\rightarrow Cr + O_2^-$	6.9	$\rightarrow Cu + O_2^-$	3.6
$NiO_2 \rightarrow Ni + O_2$	2.4	2.47 ± 0.43[g]	$\rightarrow Cr^- + O_2$	7.1	$\rightarrow CuO^- + O$	5.1
$\rightarrow NiO + O$	3.6		$\rightarrow CrO^- + O$	7.4	$\rightarrow CuO + O^-$	5.2
$CuO_2 \rightarrow Cu + O_2$	0.8	0.65 ± 0.22[g]	$CuO_2^- \rightarrow CuO + O^-$	5.5	$ZnO_2^- \rightarrow Zn + O_2^-$	2.2
$\rightarrow CuO + O$	3.5		$\rightarrow Cu + O_2^-$	6.2	$\rightarrow Zn + O_2 + e$	2.6[h]
$ZnO_2 \rightarrow Zn + O_2$	−0.6		$\rightarrow Cu^- + O_2$	6.6	$\rightarrow ZnO^- + O$	4.6
$\rightarrow ZnO + O$	3.5		$\rightarrow CuO^- + O$	7.1	$\rightarrow ZnO + O^-$	5.1

[a] See ref 91. [b] See refs 92−94. [c] See ref 95. [d] See ref 96. [e] See refs 97 and 98. [f] See ref 99. [g] See ref 100. [h] Zn has zero electron affinity.[101]

and ZnO_2^- are more stable thermodynamically as well. For the rest of the anions, the topmost decay channel corresponds to detachment of an extra electron.

Summary

Our self-consistent calculations of the electronic and geometrical structure of different isomers of 3d-metal dioxides and their anions show many interesting features:

(i) All the neutral dioxides and their anions prefer to form ground states of the oxo form except for copper dioxide, whose ground state has a superoxo form.

(ii) Inside each isomeric form, oxo, peroxo, or superoxo, the dioxides and their anions possess a large number of closely spaced spin multiplet structures.

(iii) Many dioxide anions possess several states stable toward autodetachment of an extra electron and fragmentation. For example, FeO_2^- has five stable states within an energy range of 0.35 eV. The nickel dioxide anion has three states of an oxo form, three states of a peroxo form, and two states of a superoxo form stable toward autodetachment and fragmentation.

(iv) The energy gap between peroxo, superoxo, and oxo forms decreases when moving from TiO_2 to ZnO_2. For copper dioxide, the superoxo CuOO is more stable than the linear CuO_2 lowest energy oxo state.

(v) Inside each oxo, peroxo, and superoxo groups of neutral isomers, the lowest energy isomers are able to attach an extra electron and form an anion state stable toward autodetachment to the corresponding neutral parent.

(vi) Peroxo anion states have been observed in photodetachment spectra for $ScO_2^-/Sc(O_2)^-$, $NiO_2^-/Ni(O_2)^-$, and $CuO_2^-/Cu(O_2)^-$. Our computed values of detachment energies of an extra electron from these peroxo states are in good agreement with experiment.

(vii) In many cases, the peroxo or superoxo O_2 group carries no essential spin density. The spin multiplicities of the lowest energy peroxo and superoxo isomers are the same as those of the corresponding 3d-metal ground-state dioxides, except for $Co(O_2)$ and NiOO.

(viii) The peroxo isomers prefer to form low-spin multiplicity states of the anions upon attachment of an extra electron, while the superoxo isomers prefer to form high-spin multiplicity states. Thus, the peroxo anion isomers have the same spin multiplicities as the corresponding ground-state 3d-metal monoxides.

(ix) All the ground-state 3d-metal dioxides and their anions are stable toward fragmentation except for ZnO_2, which is unstable toward evolution of molecular oxygen. The most stable system in the neutral series is TiO_2. All the ground-state anions are more stable toward fragmentation than their neutral parents. In addition, the anions NiO_2^-, CuO_2^-, and ZnO_2^- are thermodynamically more stable than their neutral parents.

Acknowledgment. This work was supported in part by a grant from the Department of Energy (DE-FG05−96ER45579). We thank Dr. L. S. Wang for providing us with his unpublished data, valuable comments, and discussions.

References and Notes

(1) Rao, C. N. R.; Raveau, B. *Transition metal oxides*; VCH Publishers: New York, 1995.

(2) Cox, P. A. *Transition metal oxides*; Oxford University Press: New York, 1992.

(3) *Homogeneous transition metal catalized reactions*; Moser, W. R., Scolum, D. W., Eds.; American Chemical Society: Washington, DC, 1992.

(4) Bell, R. C.; Zemski, K. A.; Castleman, A. W., Jr. *J. Phys. Chem. A* **1998**, *102*, 8293.

(5) Bell, R. C.; Zemski, K. A.; Castleman, A. W., Jr. *J. Phys. Chem. A* **1999**, *103*, 2992.

(6) Huber, K. P.; Herzberg, G. *Constants of Diatomic Molecules*; Van Nostrand-Reinhold: New York, 1979.

(7) Merer, A. J. *Annu. Rev. Phys. Chem.* **1989**, *40*, 407.

(8) Weltner, W., Jr.; McLeod, D. *J. Chem. Phys.* **1965**, *69*, 3488.

(9) McIntyre, N. S.; Thompson, K. R.; Weltner, W., Jr. *J. Phys. Chem.* **1971**, *75*, 3243.

(10) DeVore, T. C.; Gallaher, T. N. *High. Temp. Sci.* **1983**, *16*, 269.

(11) Ferrante, R. F.; Wilkerson, J. L.; Fraham, W. R. M.; Weltner, W., Jr. *J. Chem. Phys.* **1977**, *67*, 5904.

(12) Howard, J. A.; Sutcliffe, R.; Mile, B. *J. Phys. Chem.* **1984**, *88*, 4351.

(13) Kasai, P. H.; Jones, P. M. *J. Phys. Chem.* **1986**, *90*, 4239.

(14) Van Zee, R. J.; Hamrick, Y. M.; Li, S.; Weltner, W., Jr. *Chem. Phys. Lett.* **1992**, *195*, 214.

(15) Van Zee, R. J.; Hamrick, Y. M.; Li, S.; Weltner, W., Jr. *J. Phys. Chem.* **1992**, *96*, 7247.

(16) Huber, H.; Klotzbücher, W.; Ozin, G. A.; Voet, A. Van der. *Can. J. Chem.* **1973**, *51*, 2722.

(17) Abramowitz, S.; Acquista, N. *Chem. Phys. Lett.* **1977**, *50*, 423.

(18) Almond, M. J.; Hahne, M. *J. Chem. Soc., Dalton Trans.* **1988**, 2255.

(19) Bauschlicher, C. W., Jr.; Zhou, M.; Andrews, L.; Johnson, J. R. T.; Panas, I.; Snis, A.; Roos, B. O. *J. Phys. Chem. A* **1999**, *103*, 5463.
(20) Rosi, M.; Bauschlicher, C. W., Jr.; Chertihin, G. V.; Andrews, L. *Theor. Chem. Acc.* **1998**, *99*, 106.
(21) Chertihin, G. V.; Andrews, L.; Rosi, M.; Bauschlicher, C. W., Jr. *J. Phys. Chem. A* **1997**, *101*, 9085.
(22) Chertihin, G. V.; Andrews, L. *J. Phys. Chem.* **1995**, *99*, 6356.
(23) Chertihin, G. V.; Bare, W. D.; Andrews, L. *J. Phys. Chem. A* **1997**, *101*, 5090.
(24) Chertihin, G. V.; Bare, W. D.; Andrews, L. *J. Chem. Phys.* **1997**, *107*, 2798.
(25) Chertihin, G. V.; Andrews, L. *J. Phys. Chem.* **1997**, *101*, 8547.
(26) Chertihin, G. V.; Saffel, W.; Yustein, J. T.; Andrews, A.; Neurock, M.; Ricca, A.; Bauschlicher, C. W., Jr. *J. Phys. Chem.* **1996**, *100*, 5261.
(27) Chertihin, G. V.; Citra, A.; Andrews, L.; Bauschlicher, C. W., Jr. *J. Phys. Chem. A* **1997**, *101*, 8793.
(28) Citra, A.; Chertihin, G. V.; Andrews, L. *J. Phys. Chem. A* **1997**, *101*, 3109.
(29) Chertihin, G. V.; Andrews, L.; Bauschlicher, C. W., Jr. *J. Phys. Chem. A* **1997**, *101*, 4026.
(30) Chertihin, G. V.; Andrews, L. *J. Chem. Phys.* **1997**, *106*, 3457.
(31) Tevault, D. E. *J. Chem. Phys.* **1982**, *76*, 2859.
(32) Ozin, G. A.; Mitchell, S. A.; Garcìa-Prieto, J. *J. Am. Chem. Soc.* **1983**, *105*, 6399.
(33) Bondybey, V. E.; English, J. H. *J. Phys. Chem.* **1984**, *88*, 2247.
(34) Mattar, S. M.; Ozin, G. A. *J. Phys. Chem.* **1988**, *92*, 3511.
(35) Serebrennikov, L. V.; Mal'tsev, A. A. *Vestnik Mosk. Univ., Ser. 2* **1975**, *16*, 251.
(36) Wenthold, P. G.; Jonas, K. L.; Lineberger, W. C. *J. Chem. Phys.* **1997**, *106*, 9961.
(37) Darling, J. H.; Garton-Sprenger, M. B.; Ogden, J. S. *Symp. Faraday Soc.* **1974**, *8*, 75.
(38) Almond, M. J.; Downs, A. J.; Perutz, R. N. *Inorg. Chem.* **1985**, *24*, 275.
(39) Wu, H.; Wang, L. S. *J. Phys. Chem. A* **1998**, *102*, 9129.
(40) Wu, H.; Wang, L. S. *J. Phys. Chem.* **1997**, *107*, 8221.
(41) Wu, H.; Wang, L. S. *J. Chem. Phys.* **1998**, *108*, 5310.
(42) Gutsev, G. L.; Rao, B. K.; Jena, P.; Li, X.; Wang, L. S. *J. Chem. Phys.* **2000**, *113*, 1473.
(43) Fan, J.; Wang, L. S. *J. Chem. Phys.* **1995**, *102*, 8714.
(44) Wang, L. S. Personal communication.
(45) Wu, H.; Wang, L. S. *J. Chem. Phys.* **1997**, *107*, 16.
(46) Wu, H.; Desai, S. R.; Wang, L. S. *J. Phys. Chem. A* **1997**, *101*, 2103.
(47) Wang, L. S. In *Advanced Series in Physical Chemistry*; Ng, C. Y., Ed.; World Scientific Publishing Co.: Singapore, 2000; Vol. 10, Chapter XVI.
(48) Rudnyi, E. B.; Kaibicheva, E. A.; Sidorov, L. N. *J. Chem. Thermodyn.* **1993**, *25*, 929.
(49) Bauschlicher, C. W., Jr.; Maitre, P. *Theor. Chim. Acta* **1995**, *90*, 189.
(50) Noga, J.; Bartlett, R. J. *J. Chem. Phys.* **1987**, *86*, 7041.
(51) Gutsev, G. L.; Rao, B. K.; Jena, P. *J. Phys. Chem. A* **2000**, *104*, 5374.
(52) Clementi, E.; Chakravorty, S. J. *J. Chem. Phys.* **1990**, *93*, 2591.
(53) Gill, P. M. W.; Johnson, B. G.; Pople, J. A. *Int. J. Quantum Chem. Symp.* **1992**, *26*, 319.
(54) Oliphant, N.; Bartlett, R. J. *J. Chem. Phys.* **1994**, *100*, 6550.
(55) Sekino, H.; Oliphant, N.; Bartlett, R. J. *J. Chem. Phys.* **1994**, *101*, 7788.
(56) Becke, A. D. *J. Chem. Phys.* **1993**, *98*, 5648.
(57) Stevens, P. J.; Devlin, F. J.; Chablowski, C. F.; Frisch, M. J. *J. Phys. Chem.* **1994**, *98*, 11623.
(58) Walsch, M. B.; King, R. A.; Schaefer III, H. F. *J. Chem. Phys.* **1999**, *110*, 5224.
(59) Ramana, M. V.; Phillips, D. H. *J. Chem. Phys.* **1988**, *88*, 2637.
(60) Bergström, R.; Lunell, S.; Eriksson, L. A. *Int. J. Quantum Chem.* **1996**, *59*, 427.
(61) Hagfeldt, A.; Bergström, R.; Siegbahn, H. O. G.; Lunell, S. *J. Phys. Chem.* **1993**, *97*, 17275.
(62) Knight, L. B.; Babb, R.; Ray, M.; Banisauskas, III, T. J.; Russon, L.; Dailey, R. S.; Davidson, E. R. *J. Chem. Phys.* **1996**, *105*, 10237.
(63) Veliah, S.; Xiang, K. H.; Pandey, R.; Recio, J. M.; Newsam, J. M. *J. Phys. Chem.* **1998**, *102*, 1126.
(64) Dedieu, A.; Rohmer, M. M. *J. Am. Chem. Soc.* **1977**, *99*, 8050.
(65) Case, D. A.; Huynh, B. H.; Karplus, M. *J. Am. Chem. Soc.* **1979**, *101*, 4433.
(66) Andrews, L.; Chertihin, G. V.; Ricca, A.; Bauschlicher, C. W., Jr. *J. Am. Chem. Soc.* **1996**, *118*, 467.
(67) Harcourt, R. D. *Chem. Phys. Lett.* **1990**, *167*, 374.
(68) Lyne, P. D.; Mingos, D. M. P.; Ziegler, T.; Downs, A. J. *Inorg. Chem.* **1993**, *32*, 4785.
(69) Bauschliher, C. W., Jr.; Langhoff, S. R.; Patridge, H.; Sodupe, M. *J. Phys. Chem.* **1993**, *97*, 856.
(70) Blomberg, M. R. A.; Siegbahn, P. E. M.; Strich, A. *Chem. Phys.* **1985**, *97*, 287.
(71) Hrušák, J.; Koch, W.; Schwarz, H. *J. Chem. Phys.* **1994**, *101*, 3898.
(72) Mochizuki, Y.; Tanaka, K.; Kashiwagi, H. *Chem. Phys.* **1991**, *151*, 11.
(73) Mochizuki, Y.; Nagashima, U.; Yamamoto, S.; Kashiwagi, H. *Chem. Phys. Lett.* **1989**, *164*, 225.
(74) Ha, T. K.; Nguyen, M. T. *J. Phys. Chem.* **1985**, *89*, 5569.
(75) Barone, V.; Adamo, C. *J. Phys. Chem.* **1996**, *100*, 2094.
(76) Gutsev, G. L.; Khanna, S. N.; Rao, B. K.; Jena, P. *J. Phys. Chem. A* **1999**, *103*, 5812.
(77) Cao, Z.; Duran, M.; Solà, M. *Chem. Phys. Lett.* **1997**, *274*, 411.
(78) Gutsev, G. L.; Reddy, B. V.; Khanna, S. N.; Rao, B. K.; Jena, P. *Phys. Rev. B* **1998**, *58*, 14131.
(79) Gutsev, G. L.; Khanna, S. N.; Rao, B. K.; Jena, P. *Phys. Rev. A* **1999**, *59*, 3681.
(80) Gutsev, G. L.; Rao, B. K.; Jena, P.; Wang, X. B.; Wang, L. S. *Chem. Phys. Lett.* **1999**, *312*, 598.
(81) Gutsev, G. L.; Rao, B. K.; Jena, P. *J. Phys. Chem. A* **1999**, *103*, 10819.
(82) Schröder, D.; Fiedler, A.; Schwarz, J.; Schwarz, H. *Inorg. Chem.* **1994**, *33*, 5094.
(83) Becke, A. D. *Phys. Rev. A* **1988**, *38*, 3098.
(84) Perdew, J. P.; Wang, Y. *Phys. Rev. B* **1991**, *45*, 13244.
(85) Lee, C.; Yang, W.; Parr, R. G. *Phys. Rev. B* **1988**, *37*, 785.
(86) Wachters, A. J. H. *J. Chem. Phys.* **1970**, *52*, 1033.
(87) Hay, P. J. *J. Chem. Phys.* **1977**, *66*, 4377.
(88) Frisch, M. J.; Trucks, G. W.; Schlegel, H. B.; Gill, P. M. W.; Johnson, B. G.; Robb, M. A.; Cheeseman, J. R.; Keith, T.; Petersson, G. A.; Montgomery, J. A.; Raghavachari, K.; Al-Laham, M. A.; Zakrzewski, V. G.; Ortiz, J. V.; Foresman, J. B.; Cioslowski, J.; Stefanov, B. B.; Nanayakkara, A.; Challacombe, M.; Peng, C. Y.; Ayala, P. Y.; Chen, W.; Wong, M. W.; Andres, J. L.; Replogle, E. S.; Gomperts, R.; Martin, R. L.; Fox, D. J.; Binkley, J. S.; Defrees, D. J.; Baker, J.; Stewart, J. P.; Head-Gordon, M.; Gonzalez, C.; Pople, J. A. *Gaussian 94*, Revision B.1; Gaussian, Inc.: Pittsburgh, PA, 1995.
(89) Perdew, J. P. *Phys. Rev. B* **1986**, *33*, 8822; *Phys. Rev. B* **1986**, *34*, 7406(E).
(90) Vosko, S. H.; Wilk, L.; Nusair, M. *Can. J. Chem.* **1980**, *58*, 1200.
(91) Clemmer, D. E.; Dalleska, N. F.; Armentrout, P. B. *Chem. Phys. Lett.* **1992**, *190*, 259.
(92) Farber, M.; Uy, M.; Srivastava, R. D. *J. Chem. Phys.* **1972**, *56*, 5312.
(93) Berkowitz, J.; Chupka, W. A.; Ingram, M. G. *J. Chem. Phys.* **1957**, *27*, 87.
(94) Frantseva, K. E.; Semenov, G. A. *Teplofiz. Vys. Temp.* **1969**, *7*, 55.
(95) Grimley, R. T.; Burns, R. P.; Inghram, M. *J. Chem. Phys.* **1961**, *34*, 664.
(96) Hildenbrand, D. L.; Lau, K. H. *J. Chem. Phys.* **1994**, *100*, 8377.
(97) Helmer, M.; Plane, J. M. C. *J. Chem. Soc., Faraday Trans.* **1994**, *90*, 395.
(98) Plane, J. M. C.; Rollason, R. J. *Phys. Chem. Chem. Phys.* **1999**, *1*, 1843.
(99) Hildenbrand, D. L. *Chem. Phys. Lett.* **1975**, *34*, 352.
(100) Mitchell, S. A. *Gas-Phase Metal reactions*; Fontijn, A., Ed.; Elsevier: Amsterdam, 1992.
(101) Hotop, H.; Lineberger, W. C. *J. Phys. Chem. Ref. Data* **1985**, *14*, 731.